Research Article

URF PUBLISHERS
connect with research world

Journal of Petroleum & Chemical Engineering

https://urfpublishers.com/journal/petrochemical-engineering

Vol: 3 & Iss: 2

Dynamics of the Ramsey-Cass-Koopmans Model

Lakshmi N Sridhar*

Chemical Engineering Department, University of Puerto Rico, Mayaguez, PR 00681-9046, USA

Citation: Sridhar LN. Dynamics of the Ramsey-Cass-Koopmans Model. *J Petro Chem Eng* 2025;3(2):99-104.

Received: 16 May, 2025; **Accepted:** 03 June, 2025; **Published:** 05 June, 2025

***Corresponding author:** Lakshmi N Sridhar, Chemical Engineering Department, University of Puerto Rico, Mayaguez, PR 00681-9046, USA

ABSTRACT

Bifurcation analysis and Mult objective nonlinear model predictive control (MNLMPC) calculations are performed on two forms of the Ramsey-Cass-Koopmans (RCK) models. The MATLAB program MATCONT was used to perform the bifurcation analysis. The MNLMPC calculations were performed using the optimization language PYOMO in conjunction with the state-of-the-art global optimization solvers IPOPT and BARON. The bifurcation analysis revealed Hopf bifurcation points and branch points in the two models. The Hopf bifurcation points were eliminated using an activation factor involving the tanh function. The branch points were beneficial because they enabled the Mult objective nonlinear model predictive control calculations to converge to the Utopia point in both problems, which is the most beneficial solution. A combination of bifurcation analysis and Mult objective nonlinear model predictive control for Ramsey-Cass-Koopmans models is the main contribution of this paper.

Keywords: Economics; Bifurcation; Optimization; Control

Background

Ramsey[1], followed much later by Cass[2] and Koopmans[3], formulated the canonical model of optimal growth for an economy with exogenous 'labor-augmenting' technological progress. This model is commonly referred to as the Ramsey-Cass-Koopmans (RCK) model. The two commonly used forms of this model are the basic model (RCK model 1) without the logistic growth rate of Labor and the model that includes the logistic growth rate of Labor(RCK model 2). Much computational research has taken place using both forms of the RCK models.

Becker and Foias[4], studied local bifurcation patterns of Ramsey equilibrium. Duczynski[5], investigated the technological diffusion in the Ramsey model. Smith[6], obtained a closed-form solution to the Ramsey model. Accinelli and Brida[7], formulated the Ramsey model of optimal growth with the Richards population growth law. Accinelli, Brida[8] and Brida and Accinelli[9], studied the Ramsey model with logistic population growth. Barnett and Duzhak[10], studied non-robust dynamic inferences from macro econometric models, demonstrating the bifurcation of confidence regions. Ferrara and Gurrini[11,12], investigated the Ramsey model with logistic population growth and Benthamite felicity function.

Barnett and Duzhak[13], assessed bifurcation regions within new Keynesian models. Banerjee, et al[14], performed a bifurcation analysis of Zellner's Marshallian macroeconomic model. Guerrini[15], discovered a Hopf bifurcation in a delayed Ramsey model with von Bertalanffy population law. Barnett and Eryilmaz[16], conducted an analytical and numerical search for bifurcations in an open economy new Keynesian model. Asare, et al[17], performed bifurcation analysis studies of the Ramsey-Cass-Koopmans growth models.

This work aims to perform bifurcation analysis and Mult objective nonlinear model predictive control on the Ramsey-Cass-Koopmans model (RCK model 1) without the logistic

growth rate of labor and the model that includes the logistic growth rate of Labor (RCK model 2). The paper is organized as follows. First, the two RCK models are presented. The numerical procedures (bifurcation analysis and Mult objective nonlinear model predictive control (MNLMPC) are then described. This is followed by the results and discussion and conclusions.

RCK model without the logistic growth rate of Labor (RCK model 1)

The differential equations in this model are

$$\frac{dk}{dt} = k^{\alpha} - c - \left((\delta + n + g)k\right)$$
$$\frac{dc}{dt} = (1/\theta)\left(\alpha k^{\alpha-1} - \rho - \delta - (g\theta)\right)c$$

while the base parameter values are

$$\alpha = 0.3;\ \delta = 0.05;\ \rho = 0.0667;\ \theta = 2.0;\ g = 0.02; n = 0.0056;$$

k is capital, c is the household consumption. The parameters are depreciation(δ), growth rate of labour(n), discount rate(ρ), coefficient of relative risk aversion (θ), elasticity of capital in production (α) and growth of technology(g).

RCK model with the logistic growth rate of Labor (RCK model 2)

The equations in this model are

$$\frac{dk}{dt} = k^{\alpha} - c - \left((\delta + n + g)k\right)$$
$$\frac{dc}{dt} = (1/\theta)\left(\alpha k^{\alpha-1} - \rho - \delta - (g\theta)\right)c$$
$$\frac{dL}{dt} = rL(1 - \frac{L}{L_{\max}})$$
$$n = r(1 - \frac{L}{L_{\max}})$$

The parameter values are

$$\alpha = 0.3;\ \delta = 0.05;\ \rho = 0.0667;\ \theta = 2;$$
$$r = 0.01;\ L_{MAX} = 100;\ g = 0.02;$$

k is capital, c is the household consumption and L is labor. The parameters are depreciation(δ), growth rate of labour(n), discount rate(ρ), coefficient of relative risk aversion (θ), elasticity of capital in production (α) and growth of technology(g).

θ, ρ are the bifurcation parameters and control values.

Bifurcation analysis

The MATLAB software MATCONT is used to perform the bifurcation calculations. Bifurcation analysis deals with multiple steady-states and limit cycles. Multiple steady states occur because of the existence of branch and limit points. Hopf bifurcation points cause limit cycles. A commonly used MATLAB program that locates limit points, branch points and Hopf bifurcation points is MATCONT[18,19]. This program detects Limit points (LP), branch points (BP) and Hopf bifurcation points(H) for an ODE system.

$$\frac{dx}{dt} = f(x, \alpha)$$

$x \in R^n$ Let the bifurcation parameter be α Since the gradient is orthogonal to the tangent vector,

The tangent plane at any point $W = [w_1, w_2, w_3, w_4, ...w_{n+1}]$ must satisfy

$$Aw = 0$$

Where A is

$$A = [\partial f / \partial x \quad | \partial f / \partial \alpha]$$

where $\partial f / \partial x$ is the Jacobian matrix. For both limit and branch points, the matrix $[\partial f / \partial x]$ must be singular. The n+1 th component of the tangent vector $w_{n+1} = 0$ for a limit point (LP)and for a branch point (BP) the matrix $\begin{bmatrix} A \\ w^T \end{bmatrix}$ must be singular. At a Hopf bifurcation point,

$$\det(2 f_x(x, \alpha) @ I_n) = 0$$

@ indicates the BI alternate product while is the n-square identity matrix. Hopf bifurcations cause limit cycles and should be eliminated because limit cycles make optimization and control tasks very difficult. More details can be found in Kuznetsov[21,22].

Multiobjective Nonlinear Model Predictive Control (MNLMPC)

Flores Tlacuahuaz, et al[23], developed a multiobjective nonlinear model predictive control (MNLMPC) method that is rigorous and does not involve weighting functions or additional constraints. This procedure is used for performing the MNLMPC calculations Here $\sum_{t_{i=0}}^{t_i=t_f} q_j(t_i)$ (j=12..n) represents the variables that need to be minimized/maximized simultaneously for a problem involving a set of ODE.

$$\frac{dx}{dt} = F(x, u)$$

t_f being the final time value and n the total number of objective variables and. u the control parameter. This MNLMPC procedure first solves the single objective optimal control problem independently optimizing each of the variables $\sum_{t_{i=0}}^{t_i=t_f} q_j(t_i)$ individually. The minimization/maximization of $\sum_{t_{i=0}}^{t_i=t_f} q_j(t_i)$ will lead to the values q_j^*. Then the optimization problem that will be solved is

$$\min(\sum_{j=1}^{n}(\sum_{t_{i=0}}^{t_i=t_f} q_j(t_i) - q_j^*))^2$$
$$subject\ to\ \frac{dx}{dt} = F(x, u);$$

This will provide the values of u at various times. The first obtained control value of u is implemented and the rest are discarded. This procedure is repeated until the implemented and the first obtained control values are the same or if the Utopia point where ($\sum_{t_{i=0}}^{t_i=t_f} q_j(t_i) = q_j^*$ for all j) is obtained.

Pyomo[24], is used for these calculations. Here, the differential equations are converted to a Nonlinear Program (NLP) using the orthogonal collocation method The NLP is solved using IPOPT[25] and confirmed as a global solution with BARON[26].

The steps of the algorithm are as follows

Optimize $\sum_{t_{i=0}}^{t_i=t_f} q_j(t_i)$ and obtain q_j^* at various time intervals t_i. The subscript i is the index for each time step.

Minimize $(\sum_{i=1}^{n}(\sum_{t_{i=0}}^{t_i=t_f} q_j(t_i)-q_j^*))^2$ and get the control values for various times.

Implement the first obtained control values.

Repeat steps 1 to 3 until there is an insignificant difference between the implemented and the first obtained value of the control variables or if the Utopia point is achieved. The Utopia point is when $\sum_{t_{i=0}}^{t_i=t_f} q_j(t_i)=q_j^*$ for all j.

Sridhar[27], proved that the MNLMPC calculations to converge to the Utopia solution when the bifurcation analysis revealed the presence of limit and branch points. This was done by imposing the singularity condition on the co-state equation[28]. If the minimization of q_1 lead to the value q_1^* and the minimization of q_2 lead to the value q_2^* The MNLPMC calculations will minimize the function $(q_1-q_1^*)^2+(q_2-q_2^*)^2$. The multiobjective optimal control problem is

$$\min \quad (q_1-q_1^*)^2+(q_2-q_2^*)^2 \quad subject\ to \quad \frac{dx}{dt}=F(x,u)$$

Differentiating the objective function results in

$$\frac{d}{dx_i}((q_1-q_1^*)^2+(q_2-q_2^*)^2)=2(q_1-q_1^*)\frac{d}{dx_i}(q_1-q_1^*)+2(q_2-q_2^*)\frac{d}{dx_i}(q_2-q_2^*)$$

The Utopia point requires that both $(q_1-q_1^*)$ and $(q_2-q_2^*)$ are zero. Hence

$$\frac{d}{dx_i}((q_1-q_1^*)^2+(q_2-q_2^*)^2)=0$$

the optimal control co-state equation[28] is

$$\frac{d}{dt}(\lambda_i)=-\frac{d}{dx_i}((q_1-q_1^*)^2+(q_2-q_2^*)^2)-f_x\lambda_i;\quad \lambda_i(t_f)=0$$

λ_i is the Lagrangian multiplier. t_f is the final time. The first term in this equation is 0 and hence

$$\frac{d}{dt}(\lambda_i)=-f_x\lambda_i;\lambda_i(t_f)=0$$

At a limit or a branch point, for the set of ODE $\frac{dx}{dt}=f(x,u)$ f_x is singular. Hence there are two different vectors-values for $[\lambda_i]$ where $\frac{d}{dt}(\lambda_i)>0$ and $\frac{}{dt}(\ )\ \ 0$. In between there is a vector $[\lambda_i]$ where $\frac{d}{dt}(\lambda_i)=0$. This coupled with the boundary condition $\lambda_i(t_f)=0$ will lead to $[\lambda_i]=0$ This makes the problem an unconstrained optimization problem and the only solution is the Utopia solution.

Hopf bifurcations cause unwanted oscillatory behavior and limit cycles. The tanh activation function (where a control value u is replaced by) $(u\tanh u/\varepsilon)$ is commonly used in neural nets[29-31] and optimal control problems[32] to eliminate spikes in the optimal control profile. Hopf bifurcation points cause oscillatory behavior. Oscillations are similar to spikes and the results in Sridhar, demonstrate that the tanh factor also eliminates the Hopf bifurcation by preventing the occurrence of oscillations. Sridhar[33], explained with several examples how the activation factor involving the tanh function successfully eliminates the limit cycle causing Hopf bifurcation points. This was because the tanh function increases the time period of the oscillatory behavior, which occurs in the form of a limit cycle caused by Hopf bifurcations.

Results and Discussion

When bifurcation analysis was performed in the RCK model 1 with θ as the bifurcation parameter, a Hopf bifurcation point and a branch point were found at (k,c,θ) values of (7.163779 1.263690 -2.055001) and (40.004765 -0.000000 -4.701000). This is shown in **(Figure 1a)**. The limit cycle caused by the Hopf bifurcation point is shown in **(Figure 1b)**. When θ was modified to $\theta\tanh(\theta)$ the Hopf bifurcation point disappears **(Figure 1c)** confirming the analysis of Sridhar[33]. When ρ is the bifurcation parameter, a branch point appears at (k,c,ρ) values of (40.004765 0.000000 -0.067320) **(Figure 1d)**.

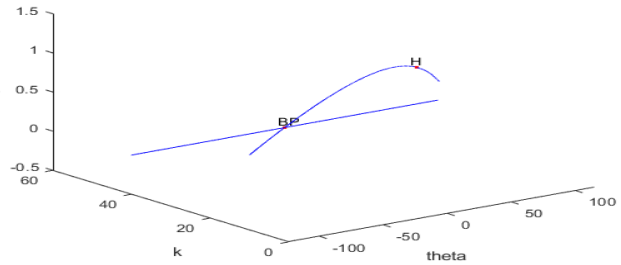

Figure 1a: (Branch point and Hopf for RCK model 1 is bifurcation parameter).

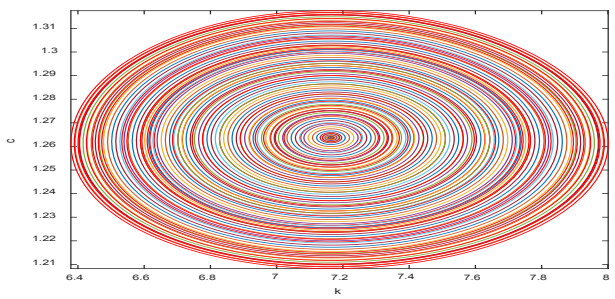

Figure 1b: (limit cycle in RCK Model 1).

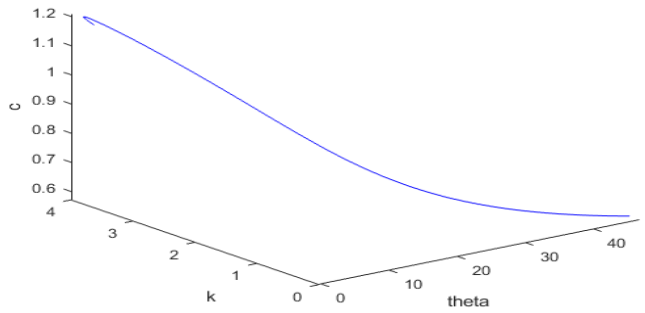

Figure 1c: (Hopf bifurcation point disappears when tanh activation factor is used in RCK model 1)

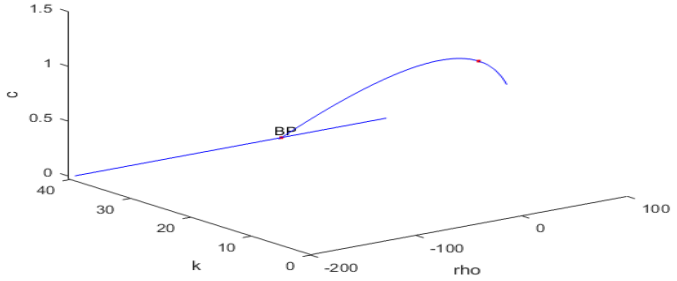

Figure 1d: (Branch point in RCK model 1 when is bifurcation parameter).

When bifurcation analysis was performed in the RCK model 2 with θ as the bifurcation parameter, a branch point was found at (k, c, L, θ) values of (36.898975 0.000000 -0.000000 -4.635000) **(Figure 2a)** and a Hopf bifurcation point was found at (k, c, L, θ) values of (6.607615 1.233421 -0.000000 -1.835001) **(Figure 2b)**. The limit cycle caused by the Hopf bifurcation point is shown in **(Figure 2c)**. When θ was modified to $\theta \tanh(\theta)/100$ the Hopf bifurcation point disappears **(Figure 2d)** confirming the analysis of Sridhar(2024b) . When ρ is the bifurcation parameter, a branch point appears at (k, c, L, ρ) values of BP (36.898975 0.000000 -0.000000 -0.066000) **(Figure 2e)**.

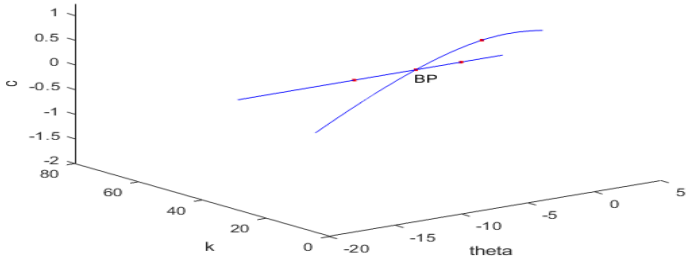

Figure 2a: (Branch point for RCK model 2 is bifurcation parameter).

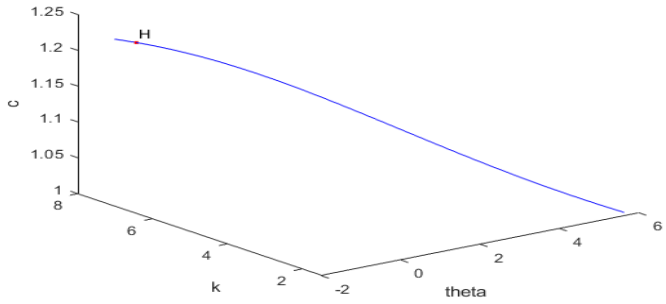

Figure 2b: (Hopf bifurcation point for RCK model 2 is bifurcation parameter).

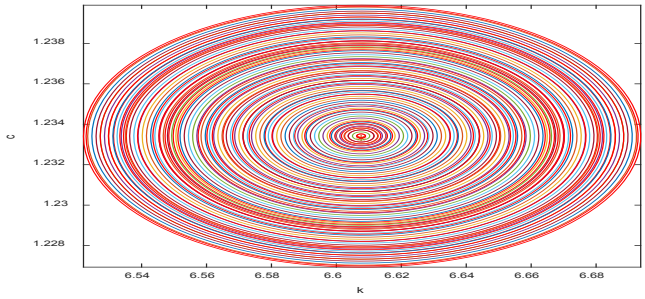

Figure 2c: (limit cycle in RCK Model 2).

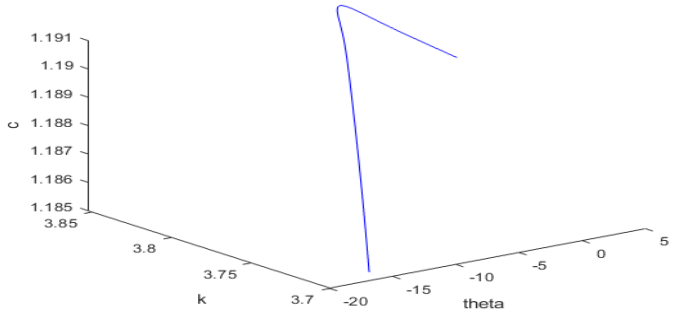

Figure 2d: Hopf bifurcation point disappears when tanh activation factor is used in RCK model 1.

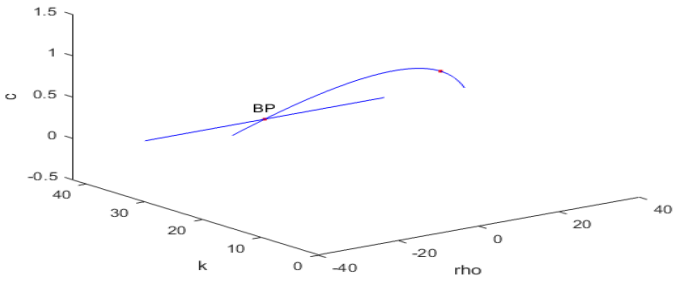

Figure 2e: Branch point in RCK model 2 when is bifurcation parameter.

When the MNLMPC calculations were performed for the RCK model 1, $\sum_{t_i=0}^{t_i=t_f} k_j(t_i)$ was minimized leading to a value of 0 and $\sum_{t_i=0}^{t_i=t_f} c_j(t_i)$ was maximized leading to a value of 20. The overall optimal control problem will involve the minimization of $(\sum_{t_i=0}^{t_i=t_f} k_j(t_i) - 0)^2 + (\sum_{t_i=0}^{t_i=t_f} c_j(t_i) - 20)^2$ was minimized subject to the equations governing the RCK model 1. This led to a value of zero (the Utopia solution. The Utopia point in the MNLMPC calculations confirms the analysis of Sridhar[27], which demonstrates that the MNLMPC calculations result in the Utopia solution when the model exhibits a branch point. The first of the control variables is implemented and the rest are discarded. This confirms the analysis of Sridhar, when the model exhibits a branch point. The process is repeated until the difference between the first and second values of the control variables are the same. The MNLMPC control values of $\theta; \rho$ obtained were (0.118, 6.741). The various MNLMPC profiles are shown in **(Figure 3a)**. The obtained control profiles exhibited noise **(Figure 3b)**. This was remedied using the Savitzky-Golay Filter.

The smoothed-out version of this profile is shown in **(Figure 3c)**.

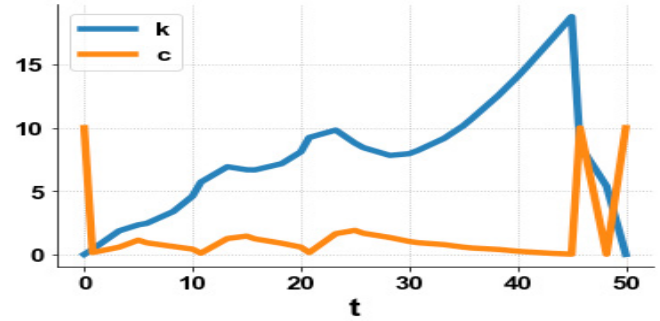

Figure 3a: k c MNLMPC profiles in RCK model 1.

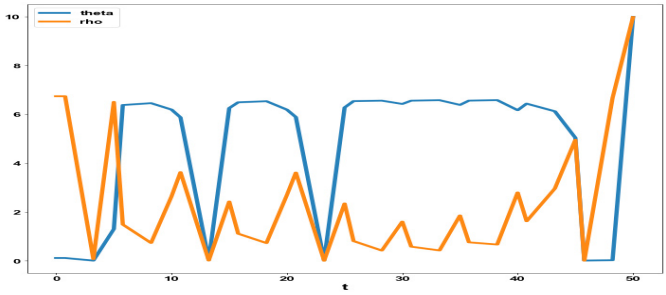

Figure 3b: Noisy MNLMPC control profiles in RCK model 1.

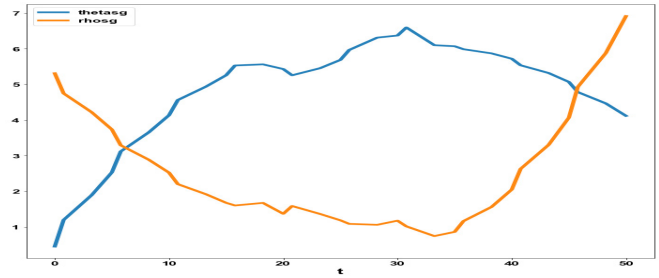

Figure 3c: Smooth MNLMPC control profiles in RCK model 1 with Savitzky Golay filter.

When the MNLMPC calculations were performed for the RCK model 2, $\sum_{t_i=0}^{t_i=t_f} k_j(t_i)$ was minimized leading to a value of 0 and $\sum_{t_i=0}^{t_i=t_f} c_j(t_i)$ was maximized leading to a value of 20. The overall optimal control problem will involve the minimization of $(\sum_{t_i=0}^{t_i=t_f} k_j(t_i)-0)^2+(\sum_{t_i=0}^{t_i=t_f} c_j(t_i)-20)^2$ was minimized subject to the equations governing the RCK model 1. This led to a value of zero (the Utopia solution. The Utopia point in the MNLMPC calculations confirms the analysis of Sridhar[27], which demonstrates that the MNLMPC calculations result in the Utopia solution when the model exhibits a branch point. The first of the control variables is implemented and the rest are discarded. The process is repeated until the difference between the first and second values of the control variables are the same. The MNLMPC control values of $\theta;\rho$ obtained were (0.118, 6.741). The various MNLMPC profiles are shown in **(Figures 3a and 3b)**. The obtained control profiles exhibited noise **(Figure 3b)**. This was remedied using the Savitzky-Golay Filter. The smoothed-out version of this profile is shown in **(Figure 3c)**.

When the MNLMPC calculations were performed for the RCK model 2, $\sum_{t_i=0}^{t_i=t_f} k_j(t_i)$ was minimized leading to a value of 0. $\sum_{t_i=0}^{t_i=t_f} c_j(t_i)$ and $\sum_{t_i=0}^{t_i=t_f} L_j(t_i)$ was maximized leading to values of 20 and 200. The overall optimal control problem will involve the minimization of $(\sum_{t_i=0}^{t_i=t_f} k_j(t_i)-0)^2+(\sum_{t_i=0}^{t_i=t_f} c_j(t_i)-20)^2+(\sum_{t_i=0}^{t_i=t_f} L_j(t_i)-200)^2$ was minimized subject to the equations governing the RCK model 1. This led to a value of zero (the Utopia solution. The Utopia point in the MNLMPC calculations confirms the analysis of Sridhar, which demonstrates that the MNLMPC calculations result in the Utopia solution when the model exhibits a branch point. The first of the control variables is implemented and the rest are discarded. The process is repeated until the difference between the first and second values of the control variables are the same. The MNLMPC control values of $\theta;\rho$ obtained were (0.107, 6.742). The various MNLMPC profiles are shown in **(Figures 4a and 4b)**. The obtained control profiles exhibited noise **(Figure 4b)**. This was remedied using the Savitzky-Golay Filter. The smoothed-out version of this profile is shown in **(Figure 4c)**.

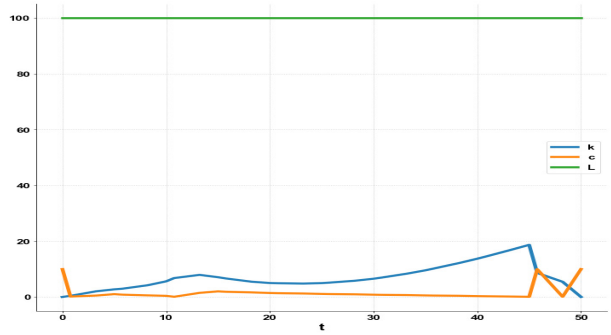

Figure 4a: k c L MNLMPC profiles in RCK model 1.

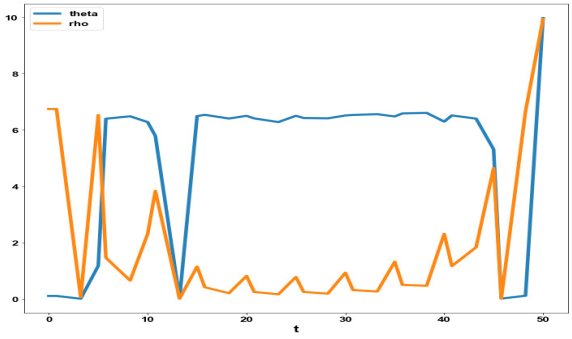

Figure 4b: Noisy MNLMPC control profiles in RCK model 2.

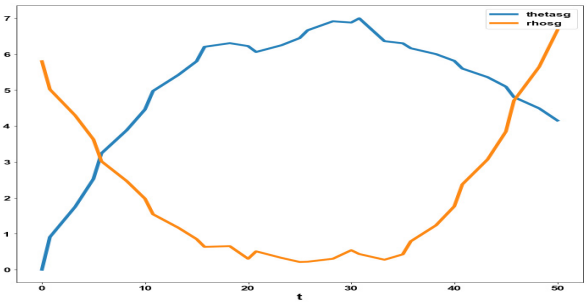

Figure 4c: Smooth MNLMPC control profiles in RCK model 2 with Savitzky Golay filter.

In both cases, the MNLMPC calculations converged to the Utopia solution, Sridhar[31], which showed that the presence of a limit or branch point enables the MNLMPC calculations to reach the best possible (Utopia) solution. Both problems exhibited limit cycles causing Hopf bifurcation points, which were successfully eliminated using an activation factor involving the tanh function, confirming the analysis of Sridhar[37]. Sridhar[37], explained with several examples how the activation factor involving the tanh function successfully eliminates the limit cycle causing Hopf bifurcation points by increasing the period of the oscillatory behavior, which occurs in the form of a limit cycle.

Conclusion

Multiobjective nonlinear model predictive control calculations were performed along with bifurcation analysis on the Ramsey-Cass-Koopman without and with the logistic growth of labor equation. The bifurcation analysis revealed the existence of Hopf bifurcation points and branch points. The Hopf bifurcation points cause unwanted limit cycles and were eliminated using a tanh activation factor. The branch points (which produced multiple steady-state solutions originating from a singular point) are very beneficial as they caused the multiojective nonlinear model predictive calculations to converge to the Utopia point (the best possible solution) in both models. A combination of bifurcation analysis and multiobjective nonlinear model predictive control for the Ramsey-Cass-Koopman models is the main contribution of this paper.

References

1. Ramsey FP. A mathematical theory of saving. The Economic J 1928;38(152):543-559.
2. Cass D. Optimum growth in an aggregative model of capital accumulation. The Review of Economic Studies 1965;32(3):233-240.
3. Koopmans TC. On the concept of optimal economic growth. The Econometric Approach to Development Planning. North-Holland, Amsterdam 1965.
4. Becker RA, Foias C. The local bifurcation of Ramsey equilibrium. Economic Theory 1994;4(5):719-744.
5. Duczynski P. Technological diffusion in the ramsey model. Int J Business, economics 2002;1(3):243-250.
6. Smith WT. A closed form solution to the Ramsey model. Economics Bulletin 2006;6:1- 27.
7. Accinelli E, Brida JG. Re-formulation of the Ramsey model of optimal growth with the Richards population growth law. WSEAS Transactions on Mathematics 2006;5:473-478.
8. Accinelli E, Brida JG. The Ramsey model with logistic population growth. Economics Bulletin 2007;3:1-8.
9. Brida JG, Accinelli E. The ramsey model with logistic population growth. Economics Bulletin 2007;3:1-8.
10. Barnett WA, Duzhak EA. Non-robust dynamic inferences from macro econometric models: Bifurcation of confidence regions. Physica A 2008;387(15):3817-3825.
11. Ferrara M, Gurrini L. The ramsey model with logistic population growth and Benthamite felicity function. Society Italian di economic publica 2009.
12. Ferrara M, Guerrini L. The Ramsey model with logistic population growth and Benthamite felicity function revisited. WSEAS Transactions on Mathematics 2009;8(3):97106.
13. Barnett WA, Duzhak EA. Empirical assessment of bifurcation regions within new keynesian models. Economic Theory 2010;45:99-128.
14. Banerjee S, Barnett WA, Duzhak EA, Gopalan R. Bifurcation analysis of zellner's Marshallian macroeconomic model. J Economic Dynamics, Control 2011.
15. Guerrini L. Hopf bifurcation in a delayed Ramsey model with von Bertalanffy population law. Int J Differential Equations, Applications 2012;11:81-86.
16. Barnett WA, Eryilmaz U. An analytical and numerical search for bifurcations in open economy new keynesian models. Munich Personal RePEc Archive 2012;40426.
17. Okyere A, Gabriel, Oduro FT, Fosu GO. On the Bifurcation Analysis of the Ramsey-Cass-Koopmans Growth Models. Int J Innovation in Sci, Mathematics 2014;2(1):2347-9051.
18. Dhooge A, Govearts W, Kuznetsov AY. MATCONT: A Matlab package for numerical bifurcation analysis of ODEs. ACM transactions on Mathematical software 2003;29(2):141-164.
19. Dhooge A, Govaerts W, Kuznetsov YA, et al. CL_MATCONT A continuation toolbox in Matlab 2004.
20. Kuznetsov YA. Laminar-Turbulent Bifurcation Scenario in 3D Rayleigh-Benard Convection Problem. Elements of applied bifurcation theory. Springer, NY 1998.
21. Kuznetsov YA. Five lectures on numerical bifurcation analysis. Utrecht University, NL 2009.
22. Govaerts wJF. Numerical Methods for Bifurcations of Dynamical Equilibria. SIAM 2000.
23. Flores-Tlacuahuac A. Pilar Morales and Martin Riveral Toledo Multiobjective Nonlinear model predictive control of a class of chemical reactors. I & EC res 2012:5891-5899.
24. William EH, Laird CD, Watson JP, et al. Pyomo - Optimization Modeling in Python Second Edition 67.
25. Wächter A, Biegler L. On the implementation of an interior-point filter line-search algorithm for large-scale nonlinear programming. Math Program 2006;106:25-57.
26. Tawarmalani M, Sahinidis NV. A polyhedral branch-and-cut approach to global optimization. Mathematical Programming 2005;103(2):225-249,.
27. Sridhar LN. Coupling Bifurcation Analysis and Multiobjective Nonlinear Model Predictive Control. Austin Chem Eng 2024a;10(3):1107.
28. Ranjan US. Optimal control for chemical engineers. Taylor and Francis 2013
29. Dubey SR, Singh SK, Chaudhuri BB. Activation functions in deep learning: A comprehensive survey and benchmark. Neurocomputing 2022;503:92-108.
30. Kamalov AF, Safaraliev NM, Cherukuri AK, Zgheib R. Comparative analysis of activation functions in neural networks. 2021 28th IEEE Int Conf Electronics, Circuits and Systems (ICECS), Dubai, United Arab Emirates 2021:1-6.
31. Szandała T. Review and Comparison of Commonly Used Activation Functions for Deep Neural Networks 2020.
32. Sridhar LN. Bifurcation Analysis and Optimal Control of the Tumor Macrophage Interactions. Biomed J Sci, Tech Res 2023;53(5).
33. Sridhar LN. Elimination of oscillation causing Hopf bifurcations in engineering problems. J Applied Math 2024;2(4):1826.